Chapter 2

Review of Literature

2.1. RECENT PYRIMIDINE BASED ANTI-CANCER AGENTS

In 2021, Reddy *et al.,* developed the coumarin-pyrimidine conjugates as anticancer agents. A simple nucleophilic substitution reaction was performed between substituted 4-bromomethyl coumarin and thymine to obtain the designed compounds. The compounds were tested for anti-cancer activity against C6 cancer cells using MTT assay, which resulted in compound **2.1** (**Figure 2.1.**) as a potent derivative (IC_{50} = 4.85μM). However, it was found to have less potency when compared with daunorubicin (IC_{50} = 2.62μM). Furthermore, the compounds possessed a good safety index against HEK293 cells (Reddy, Kongot et al. 2021).

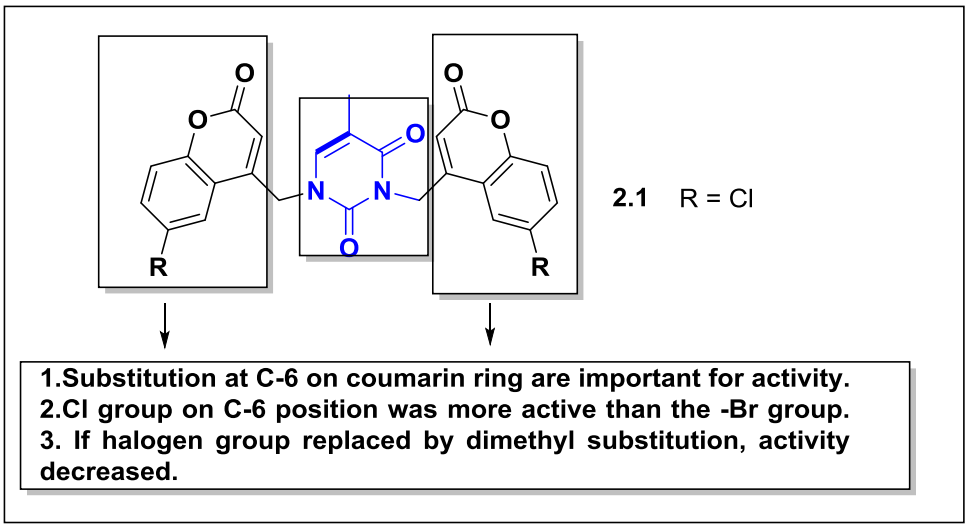

Figure 2.1. Biscoumarin–pyrimidine derivatives with anticancer activity.

Nasser *et al.*, in 2020, described a new series of pyrimidine-5-carbonitriles as anti-cancer agents targeting epidermal growth factor receptors ($EGFR^{WT}$ and $EGFR^{T790M}$) (Nasser, Eissa et al. 2020). The biological studies performed against four cancer cell lines *viz*; MCF-7 (breast cancer), HCT-116 (colon cancer), HepG-2 (liver cancer), and A549 (non-small cell lung cancer) revealed that compounds **2.2, 2.3,** and **2.4** (**Figure 2.2.**) possessed moderate anti-proliferative activity when compared to standard EGFR inhibitor, Erlotinib. Compound **2.2** showed 4.5- 8.4 times more activity than standard drug against MCF-7, HCT-116, HepG-2, and A549 cell lines showing IC_{50} values of 4.14, 3.37, 3.04, and 2.4μM respectively. Furthermore, compound **2.2** showed

inhibitory activity against both isoforms of EGFR, with IC_{50} values of 0.09µM against $EGFR^{WT}$ and 4.03µM against $EGFRT^{790M}$. *In silico* studies against EGFR suggested that the pyrimidine moiety

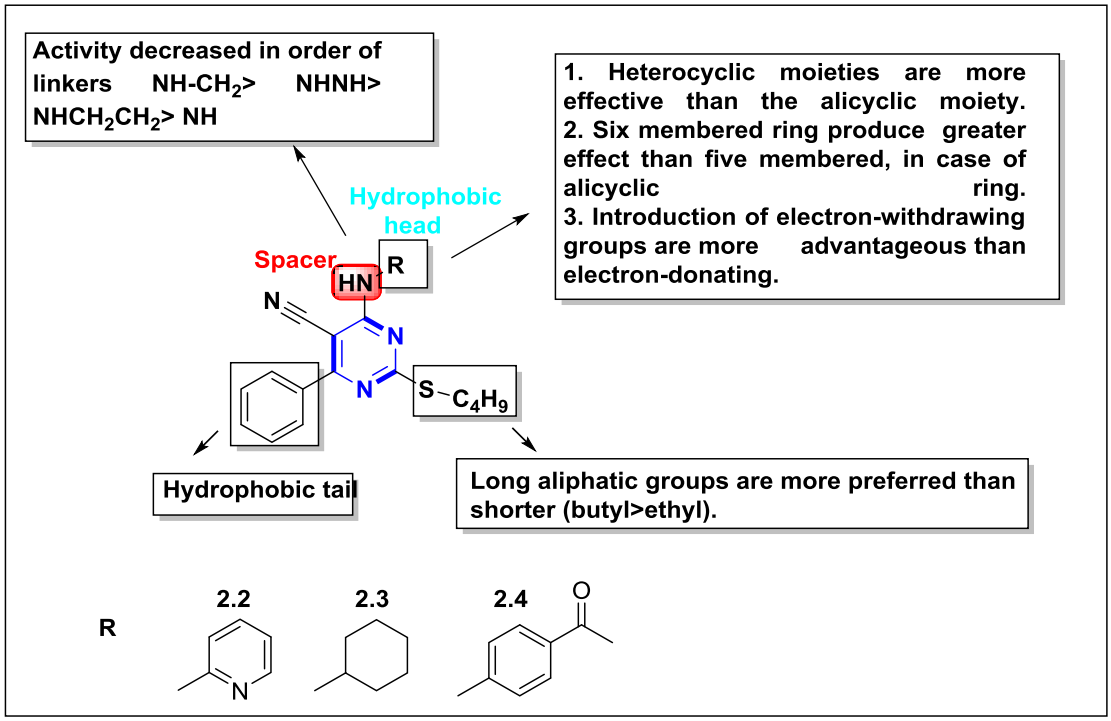

Figure 2.2. SAR analysis of pyrimidine-5-carbonitrile derivatives as anticancer agents.

of **2.2** forms H-bond interaction with Lys745, while its hydrophobic head interacts with Ala743 and Leu844 increasing the binding affinity towards the ATP-binding pocket. Moreover, SAR analysis showed that heterocycles like pyrimidine and pyridine exhibit stronger anti-cancer activity than alicyclic systems. However, in alicyclic systems, six-membered moieties fared much better than five-membered ring systems showing improved activity profile. Replacement of heterocyclic rings with non-hetero aromatic structures reduces the activity.

Kim *et al*., in 2020, developed pyrazolo[3,4-*d*]pyrimidine based small molecule heterocycles as TNF Receptor Associated Protein 1 (TRAP1) inhibitors (Kim, Kim et al. 2020). Previously, authors have reported **DN401,** a mitochondria-permeable

TRAP1 inhibitor with good anticancer activity (Park, Jeong et al. 2017). However, due to its poor metabolic stability, they attempted to design new derivatives with improved metabolic stability. A total of 60 compounds were synthesized by incorporating various substituents at the benzyl ring. From the synthesized compounds, **2.5** and **2.6** with IC_{50} =1.983µM and 0.373µM, respectively were identified as potent TRAP1 inhibitors having good metabolic and plasma stability (**Figure 2.3.**). The molecules also displayed good anti-cancer activity against many cancer cell lines including breast, liver, cervix, brain, and lung cancer. Molecular docking studies demonstrated that **2.5** and **2.6** had polar interactions with Asn119, Asp158, Thr251, and Asn171 in the binding pocket of TRAP1. Both **2.5** and **2.6** occupied lipophilic binding pockets surrounded by amino acid residues like Phe205, Met163, Ile168, Ile172, Trp231, and Ile253. *In vitro* ADME was also performed about lead compound **DN401**, suggesting compounds **2.5** and **2.6** to have better metabolic stability in rat and human microsomes.

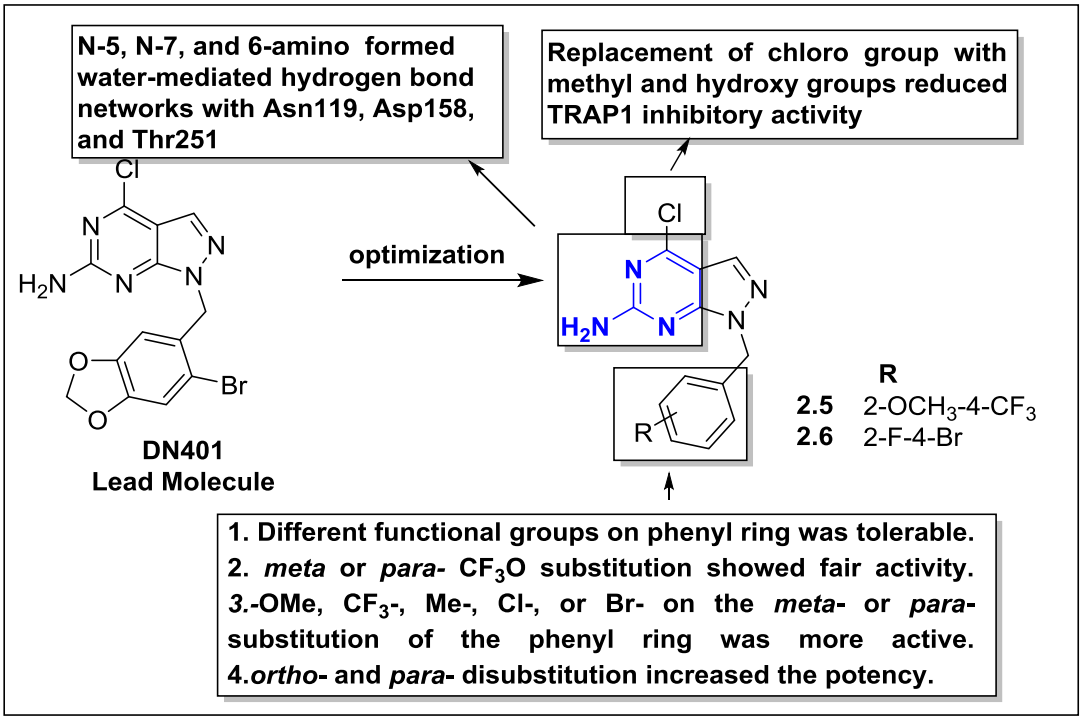

Figure 2.3. SAR profile of pyrazolo[3,4-*d*]pyrimidine based TRAP1 inhibitors.

In 2020, Farag *et al.,* reported 2,5-diamino-4 pyrimidinol analogues, synthesized by hybridization of 2-anilino-4-phenoxypyrimidines with weakly active anti-proliferative agent, 5-amino-4-pyrimidol as potential anti-proliferative agents to target M-NFS-60 cells (Farag, Hassan et al. 2020). Results of the study showed that compound **2.7** (**Figure 2.4.**) potently inhibits growth in multiple cancer cell lines such as hematological, colorectal, NSCLC, kidney, melanoma, ovarian, prostate, and breast cancer cell lines by 84.1, 72.15, 66.34, 51.55, 52.79, 66.48, 55.95, 61.85, and 60.87%, respectively. The compound **2.7** (IC_{50} = 1.97μM) also showed remarkable inhibitory activity against M-NFS-60 cells. ADME study showed that compound **2.7** possesses significant GIT permeability (P_e = 19.0 ± 1.1 × 10^{-6} cm/s). Binding mode analysis in the cavity of CSF1R displayed π-π interaction between the pyrimidine ring of **2.7** with Tyr665 and H-bond interaction with Thr663, while in the binding site of DAPK1, **2.7** occupied the hydrophobic pocket followed by orientation of methoxy substituent on phenyl ring towards the hydrophilic region and formed H-bond with Tyr240, Leu111, Leu211, Glu239, and Asn243.

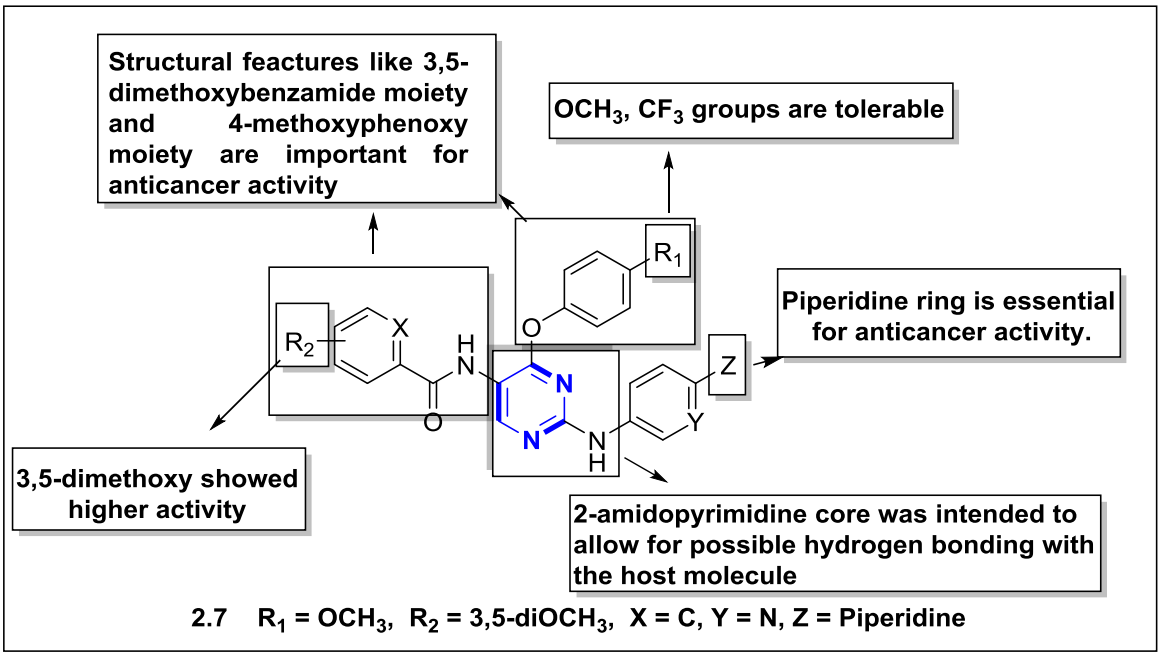

Figure 2.4. SAR analysis of 2,5-diamino-4-pyrimidinol derivatives as anti-cancer agents.

Amin *et al.*, in 2019 reported 6-aryl-5-cyano-pyrimidine derivatives as anti-tumor agents with potent inhibitory activity against thymidylate synthase (Amin, Shawer et al. 2019).The anti-cancer activity of these derivatives was tested against HePG-2, MCF-7, and HCT-116 cell lines, with 5-fluorouracil as standard. All compounds displayed significant anti-cancer activity with compound **2.8** (**Figure 2.5.**) emerging as most potent derivative. It showed IC_{50} values of 63.42µM, 50.35µM, and 36.47µM towards HePG-2, HCT-116 and MCF-7 cancer cell lines, respectively. Further, **2.8** showed thymidylate synthase (TS) inhibitory activity (70.41% TS inhibition) with IC_{50} value = 3.89nM. *In silico* studies against human thymidylate synthase protein (PDB: 6QXG) revealed that compound **2.8** forms H-bond interactions with Asn226, Asp218, and Gly222 amino acids with a binding score of -5.39 Kcal/mol.

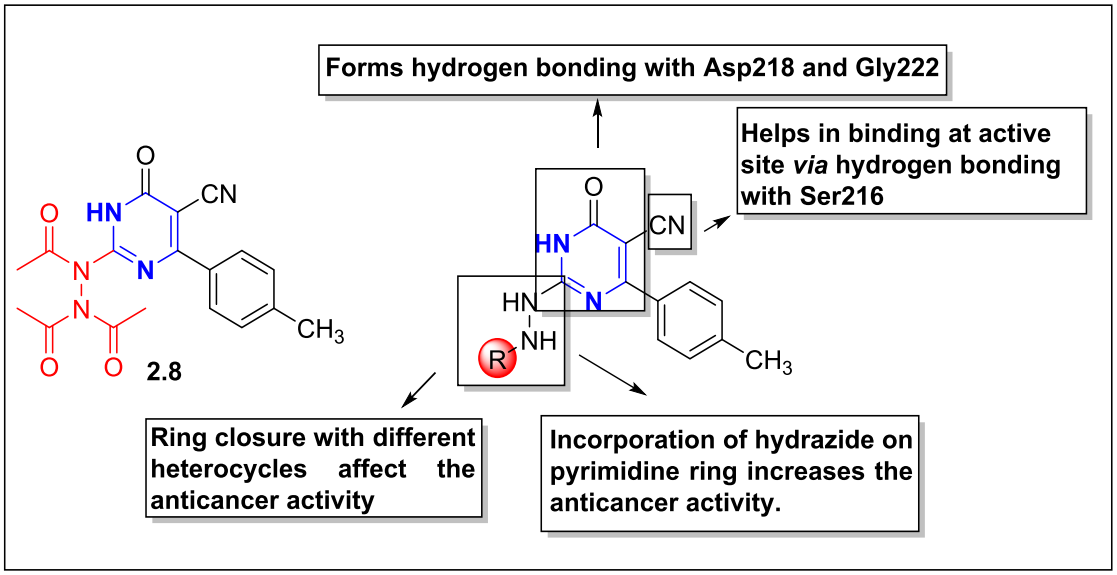

Figure 2.5. 6-aryl-5-cyano-pyrimidine derivatives as thymidylate synthase inhibitors.

In 2019, Diao *et al.,* developed benzothiazole linked pyrimidine based compounds as potent inhibitors of CDK2 (Diao, Lin et al. 2019). Upon synthesis, benzothiazole linked pyrimidine derivatives were evaluated for their anti-cancer potential against PC-3, HeLa, HCT116, and MDA-MB-231 cell lines using AZD5438 as a standard drug. Among all the derivatives, compound **2.9** with IC_{50} values of 0.92, 0.45, 0.70, and 1.80µM, respectively, exhibited noteworthy anti-cancer activity when compared

with AZD5438 (**Figure 2.6.**). The active compound **2.9** exhibited an IC_{50} value of 5.4nM against CDK2, that was three times than standard drug (IC_{50} = 45nM) and thus claimed as excellent CDK2 inhibitor. Docking studies revealed that compound **2.9** fits well into the ATP-pocket of CDK2 (PDB ID: 6GUE). The pyrimidine ring showed two H-bonds with Leu83 whereas another H-bond was showed by the sulfur atom of benzothiazole with Lys33. Further, flow cytometry analysis and cell apoptosis study displayed that compound **2.9** induced apoptosis *via* G2/M cell cycle arrest.

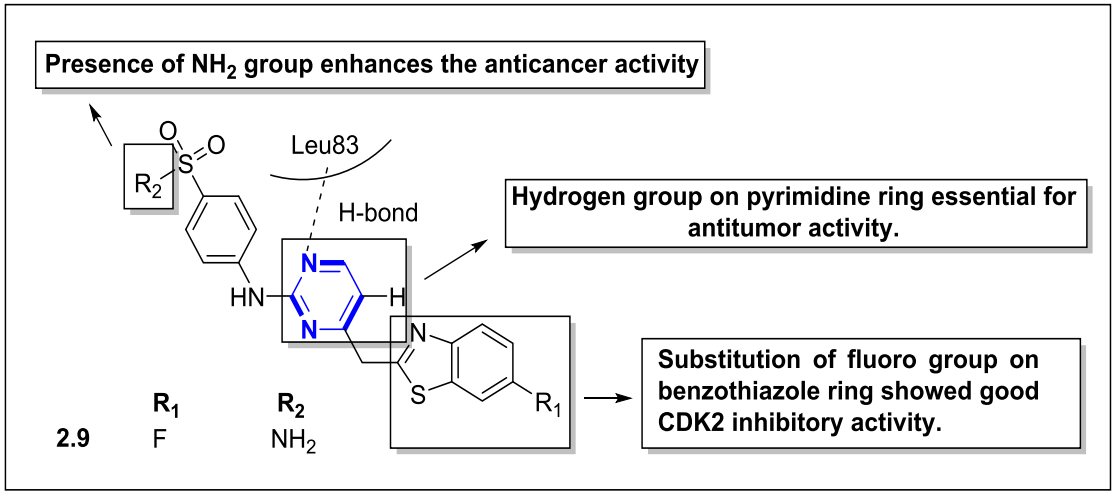

Figure 2.6. SAR analysis of benzothiazole linked pyrimidine derivatives as potential anti-cancer agents.

Kumar *et al.*, in 2018, reported the synthesis of pyrimidine bridged combretastatin analogues as anti-cancer agents (Kumar, Sharma et al. 2018). Out of all the compounds, **2.10** and **2.11** (**Figure 2.7.**) were found to possess significant anticancer activity. Against MCF7, **2.10** showed IC_{50} = 4.67µM and **2.11** showed IC_{50} = 4.63µM, while against A549, **2.10** showed IC_{50} = 3.38µM and **2.11** showed IC_{50} = 3.71µM. Compounds were also evaluated for tubulin polymerization inhibitory potential using colchicine as reference. It was observed that compound **2.10** displayed comparable inhibitory activity to that of colchicine. Further, a competitive binding assay was carried, which revealed compound **2.10** as a competitive inhibitor of the colchicine binding site. Molecular docking analysis displayed that both the compounds **2.10** and

2.11 well occupied the colchicine-binding pocket (PDB: 4O2B) in addition to the combretastatin binding pocket of the tubulin (PDB: 5LYJ). SAR analysis revealed that the presence of dichloro substituents on B ring enhances the activity. The introduction of substituents like methyl and amino group on the pyrimidine core showed significant anti-cancer activity.

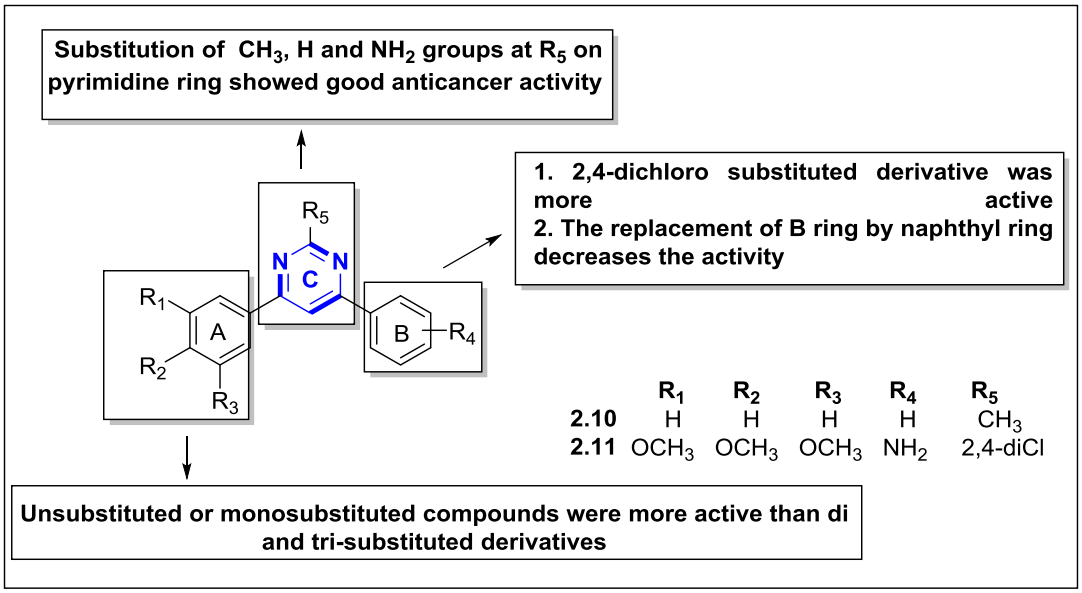

Figure 2.7. SAR analysis of pyrimidine bridged combretastatin analogues as anti-cancer agents.

Mohamed *et al.,* synthesized derivatives of 6-aryl-5-cyano thiouracil and estimated their *in vitro* anti-cancer potential against MCF-7 and HePG-2 cell lines (Mohamed, Khalil et al. 2017). From the synthesized compounds, **2.12, 2.13,** and **2.14** (**Figure 2.8.**) showed good inhibitory activity as compared to standard 5-fluorouracil. Compound **2.12** was found to be most active towards both cell lines, MCF-7 and HepG2, with IC_{50} values of 23.9µM and 25.5µM, respectively. Compound **2.13** exhibited an IC_{50} value of 25.7µM and 25.7µM whereas compound **2.14** showed IC_{50} values of 27.7µM and 24.1µM against MCF-7 and HepG2 cell lines, respectively. Furthermore, docking studies revealed that compound **2.12** scored the highest binding energy score of -42.23 Kcal/mol while **2.14** showed a score of -39.19 Kcal/mol. The carbonyl group of the pyrimidine ring of compound **2.13** interacts with His 256 *via* H-

bond and the cyano group at 5-position of pyrimidine was involved in H-bond with Asp218. In compound **2.14** acetyl group is important and showed H-bond with amino acids such as Asn226, Arg50, Asn112, Gln214, and Asp218.

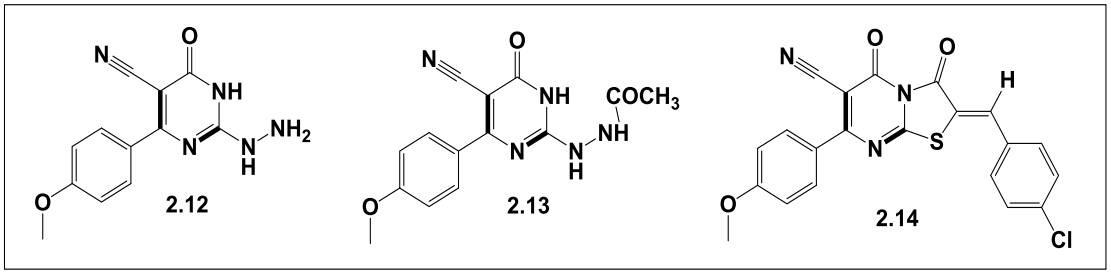

Figure 2.8. Thiouracil derivatives as potential anticancer compounds.

2.2. PYRIMIDINE DERIVATIVES AS INHIBITORS OF MAPK PATHWAY

Pyrimidine-based MAPK pathway inhibitors have also been reported in the literature. Hawala *et al.,* reported pyrimidine bearing sulphonamide scaffolds as anti-cancer agents *via* ERK inhibition. Cell lines used in the study were MCF7, HCT-116, and HepG-2. Among the synthesized compounds, **2.15** and **2.16** were found as most active compounds in comparison to the reference drugs, vinblastine and doxorubicin. Further flow cytometry and cell cycle analysis of compounds revealed that **2.15** induced apoptosis and cell cycle arrest at the G2/M phase in all the cell lines. Molecular docking analysis showed an important π-π interaction formed between pyrazolo[1,5-*a*]pyrimidine and Try36. Phenolic moiety also exhibited π-cation interaction with ammonium group of Lys54 in the ATP binding site of ERK1 (Halawa, Eskandrani et al. 2019). Another pyrimidine derivatives as effective Pan-RAF inhibitors were reported by Wang *et al*. The derivatives were evaluated against all iso forms of RAF kinases. Out of all the derivatives, compound **2.17** showed less activity towards ARAF and BRAFWT while had good inhibitory activity against CRAF and BRAFV600E kinases. Another derivative, **2.18** exhibited significant anti-proliferative activity against SK-Mel-2, A375, and COLO205 cancer cell lines harboring

BRAFV600E (**Figure 2.9.**). This compound also displayed remarkable activity against MV4-11, HepG2 and SW579 cancer cell lines harboring BRAFWT (Wang, Zhang et al. 2017).

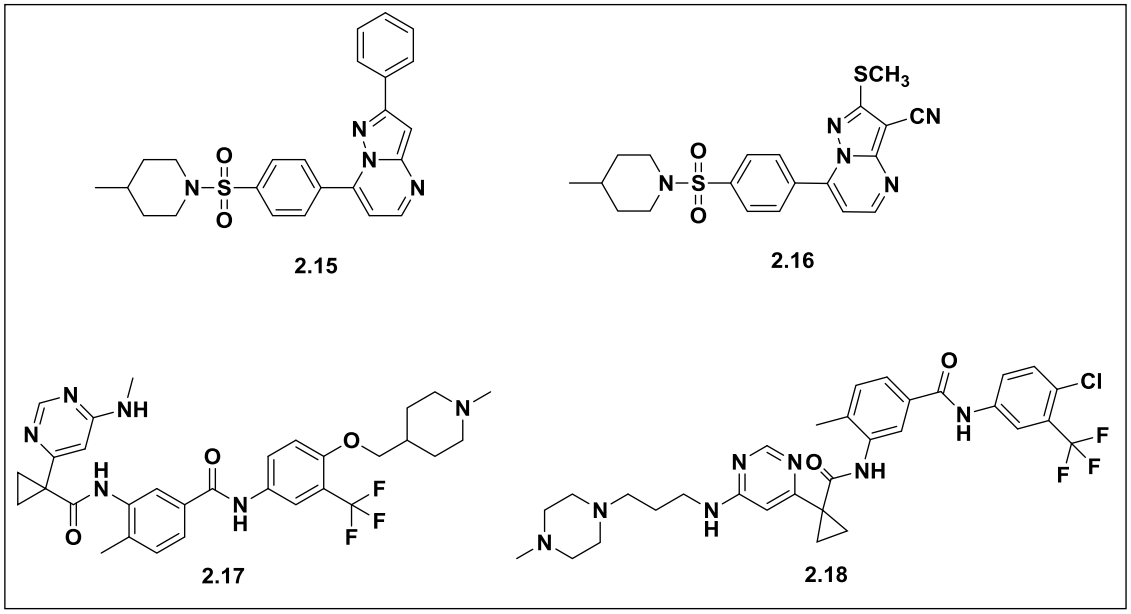

Figure 2.9. Pyrimidine derivatives as inhibitors of MAPK pathway inhibitors.

2.3. VARIOUS SMALL MOLECULE HETEROCYCLES BASED ERK1/2 INHIBITORS

The success of ERK inhibitors against different kinds of cancers has shifted the interest of many researchers toward the development of novel ERK inhibitors. Thus, continuous efforts are put to find new biologically active ERK inhibitors with more potency and less toxicity. Various reported ERK inhibitors contain various diverse chemical scaffolds such as pyrrolopyrazinone, thiazolidinone (TZD), pyrimidine, quinolone, indazole, etc.

2.3.1. Thiazolidine-2,4-dione-based inhibitors

Thiazolidinone (TZD) is a versatile scaffold with diverse pharmacological profile such as anti-cancer, anti-viral, and anti-inflammatory activity. In 2012, Liu *et al*.

designed 3,5-disubstituted-thiazolidine-2,4-dione derivatives from a lead structure that comprised of a phenyl ring, thiazolidine, and an ethylamine moiety and established them as inhibitors of the Raf/MEK/ERK pathway. The analogs were designed by incorporating different substituents like cyclohexyl, a phenyl ring, a heterocyclic ring such as pyridine and indole, and substitution of ethyl amines with groups like COOH and CH_2OH. The compounds were evaluated against cancer cell line, U937. Compounds with a benzene ring and a TZD nucleus showed good anti-proliferative activity compared to compounds that lacked an exocyclic double bond and a TZD nucleus. Compound **2.19** containing the cyclohexyl ring in place of the benzene ring exhibited three times more anticancer activity (IC_{50} = 3.4μM) than the lead structure (IC_{50} = 10.4μM) (**Figure 2.10.**). Furthermore, western blot analysis was performed for compound **2.19** and showed that it decreased the phosphorylated expression levels of ERKs at a concentration of 3μM, which indicated the correlation between growth inhibition in U937 cancer cells and blockage of ERK signaling pathway. Molecular docking studies were also performed against MEK1 (PDB: 1S9J). Compound **2.19** occupied the ATP-binding cavity with great binding affinity. The carbonyl group of TZD formed H-bonds with Lys97 and Ser194, whereas ethylamine showed interactions with Asp190, Asn195, and Asp208. SAR analysis revealed that TZD analogs bearing the phenyl ring, exocyclic double bond, and the ethylamine chain are important for anticancer activity. Electron-donating substituents (EDG) at aryl moiety enhanced the activity, whereas presence of electron-withdrawing groups (EWG) decreased the activity (Liu, Rao et al. 2012).

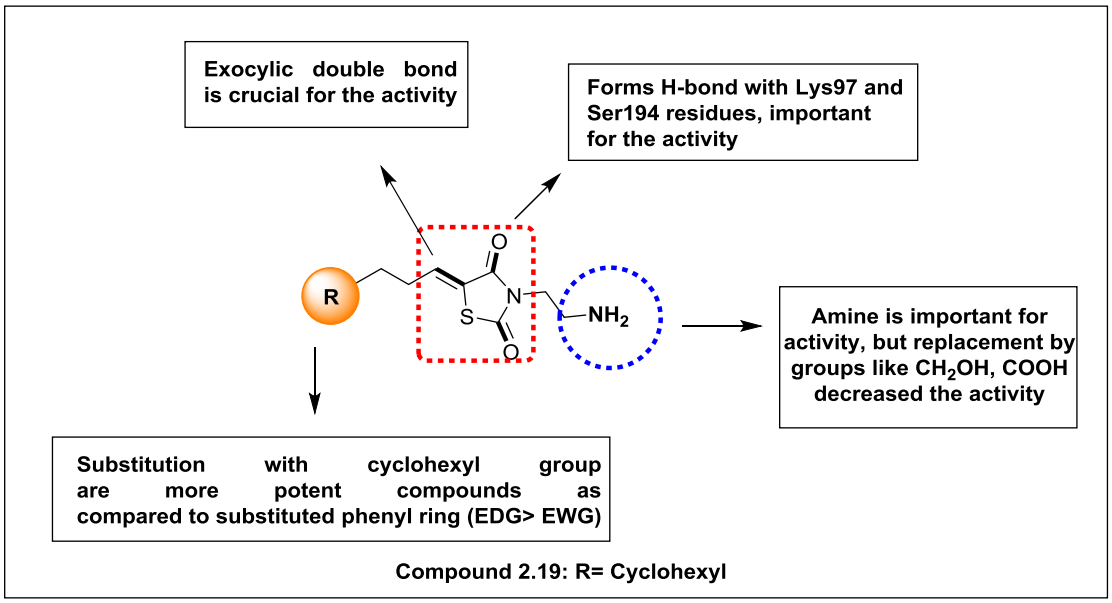

Figure 2.10. Thiazolidine-2,4-dione-based ERK inhibitors along with structure-activity relationship profile.

2.3.2. Tetrahydropyridopyrimidine-based inhibitors

In 2014, Blake *et al.,* reported the discovery of 5,6,7,8-tetrahydro-pyridopyrimidine as an ERK2 inhibitor. Combinatorial library synthesis, HTS, and molecular docking analysis identified **2.20** as a lead compound. Against HepG2 cancer cell line, **2.20** exhibited an IC_{50} value of 4.4μM by inhibiting ERK-dependent phosphorylation of p90Rsk. Docking studies established that the tetrahydro-pyridopyrimidine moiety occupied well the hydrophobic cavity of the receptor. The nitrogen of the pyrimidine ring formed H-bond with Met108 and the other groups showed interactions with residues like Lys54, Gln105, Asp167, and Glu71. Various analogs of the compound have been designed by substituting various groups at the second position of the tetrahydro-pyridopyrimidine core and in the benzylic portion to generate the SAR profile. Substitutions of the CH_2OH, chloro and fluoro groups in the benzylic portion of the compound showed good results while the substitution of tetrahydropyran (4-THP) *via* the amine linker on the tetrahydro-pyridopyrimidine core improves the potency against ERK2 and HepG2, with IC_{50} values of 1 and 45nM, respectively.

Introduction of F and Cl at the third and fourth carbon on the benzyl ring, respectively, along with the substitution of 4-THP on the tetrahydro-pyridopyrimidine core leads to the discovery of potent compound **2.21**, which exhibited a high IC_{50} of 2 and 25nM against ERK2 and HepG2, respectively (**Figure 2.11.**). *In vivo* pharmacokinetic (PK) studies evaluated against female mice, male SD (Sprague Dawley) rats, beagle dogs, and cynomolgus monkeys indicated towards acceptable pharmacokinetic profile, followed by the pharmacokinetics/pharmacodynamics (PK/PD) study in HCT116 colorectal cancer-induced nude mice. At 150mg/kg twice a day dose for twenty days, 69–95% inhibition of tumor with good tolerance was observed (Blake, Gaudino et al. 2014).

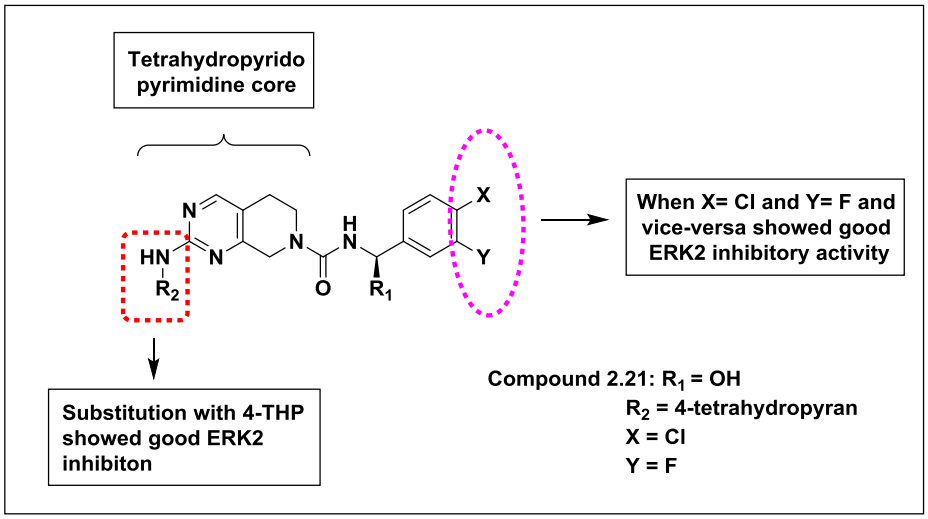

Figure 2.11. Structure-activity relationship of tetrahydro-pyridopyrimidine-based ERK2 inhibitor.

2.3.3. Coumarin-based inhibitors

In 2015, Dort *et al.,* discovered a dual inhibitor against allosteric ERKs and PI3K. The inhibitor was designed by coupling ZSTK474, a PI3K inhibitor with RO5126766, a MEK inhibitor, *via* a covalent linker. First, the 6-aminohexanamide group was attached to one of the morpholino rings of ZSTK474, and 3- chloropropyl was attached to RO5126766 using various synthetic reactions. Finally, both formed

intermediates were coupled using potassium carbonate and sodium iodide in acetonitrile to yield **2.22** (**Figure 2.12.**). This compound was further subjected to in vitro assay, and also evaluated against A549 and PANC-1 cancer lines. Results displayed that compound **2.22** exhibited potent MAPK and PI3K inhibition (IC_{50} = 473 and 172nM, respectively). Cancer cell line study also confirmed that **2.22** decreases cell viability up to 50–70% at the concentration of 10 and 25µM. In addition, molecular docking studies also established that compound **2.22** formed similar interactions as observed in RO5126766 and ZSTK474. SAR analysis displayed that the dimethylaminocarbamate group attached to the coumarin scaffold increased the ERK activity (Van Dort, Galbán et al. 2015).

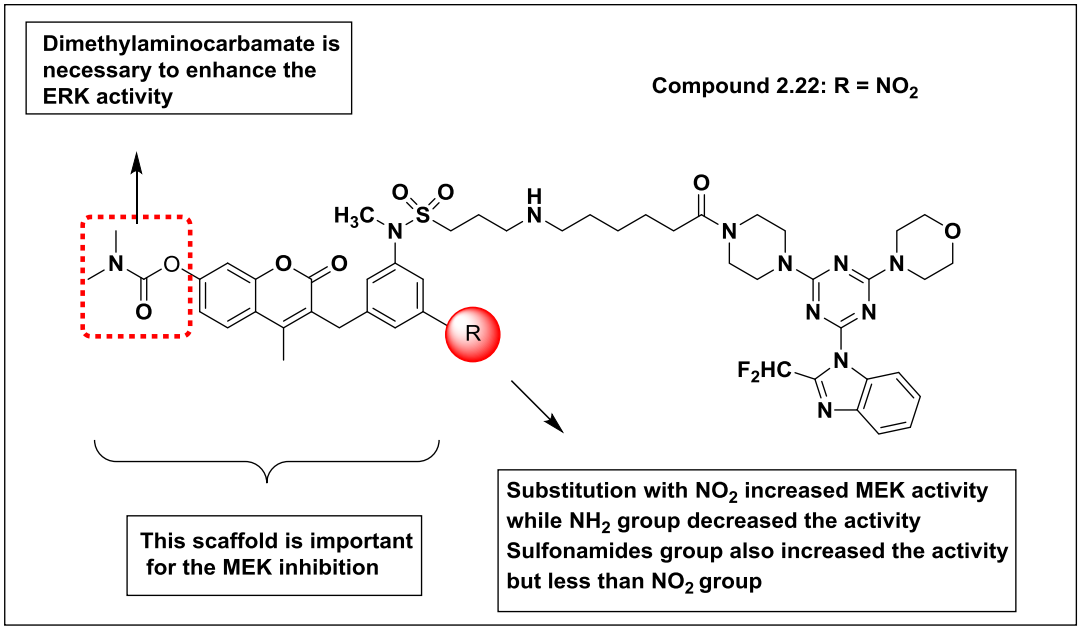

Figure 2.12. SAR profile of coumarin based inhibitors.

2.3.4. Benzhydroxamate ester-based inhibitors

In 2016, Dort *et al.,* considered compound **2.22** as the lead structure and designed various other analogs to enhance the MEK inhibitory action of previously reported inhibitors. In the new analogs, ZSTK474 (PI3K inhibitor) scaffold remained the same, while a MEK inhibitor scaffold was replaced by PD0325901 (ATP-noncompetitive

MEK inhibitor) containing benzhydroxamate ester group, which were further coupled by covalent linkers. Upon synthesis, the analogs were tested against D54 and A549 cancer cell lines, which proved that out of all the compounds, **2.23** displayed increased anti-cancer activity in the nanomolar range (IC_{50} = 0.015nM) in comparison to PD0325901 (IC_{50} = 15nM) (**Figure 2.13.**). *In vivo* study carried out on athymic nude Foxnlnu mice, induced with D54 and A549 tumors, revealed a 95% decrease in the phosphorylation of ERK1/2, thus establishing them as potent ERK inhibitors. The benzhydroxamate ester group contributed toward the increased ERK inhibition. Through molecular docking studies, it was found that compound **2.23** occupied the allosteric-binding region and both the oxygens of the hydroxamate group showed interaction with Lys97 (Van Dort, Hong et al. 2016).

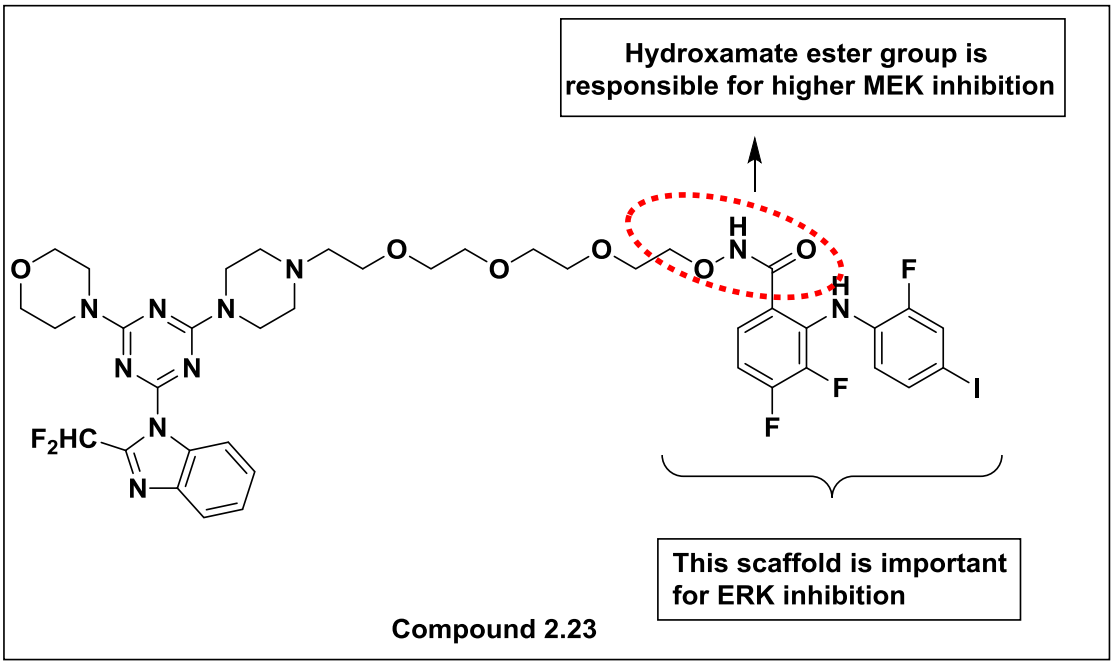

Figure 2.13. Benzhydroxamate ester-based inhibitor with SAR profile.

2.3.5. Pyridone-based inhibitors

Ren *et al.,* discovered a series of potent small molecules as ATP competitive ERK1/2 inhibitor-containing pyridine moiety. The compounds were designed by replacing the

piperidine ring of compound **2.21** with pyridine to improve the pharmacokinetic. In docking studies, it was observed that pyridine-based inhibitors occupied the same cavity and showed similar interactions with Lys 54 (H-bond with C=O of pyridine) as exhibited by compound **2.21**, and also improve the metabolic stability by removing the two metabolic spots present on the piperidinopyrimidine moiety at C-5 and C-8. The pyridine compound **2.24** containing 3-F and 4-Cl exhibited good inhibitory activity against ERK2, especially the S-enantiomeric form showed 25-times more activity compared to the R-enantiomeric form with inhibitory constant (Ki) value of 0.3 ± 0.02nM (**Figure 2.14.**). Compound **2.24** showed high permeability and no CYP450 inhibition, reflecting a better PK profile than compound **2.21**. The other PK parameters such as C_{max} (maximum concentration), clearance and AUC (area under the curve) further disclosed that clearance was less in the pyridine-based compounds compared to the previous reported piperidinopyrmidine-based compounds. PK/PD study was carried out in nude mice (induced with HCT116) revealed that it exhibits phospho-p90RSK activity with 70% inhibition. SAR analysis displayed that introduction of groups like 5-F, 5- and 6-Me on the pyridine core decreased the ERK2 inhibitory activity (Ren, Grina et al. 2015).

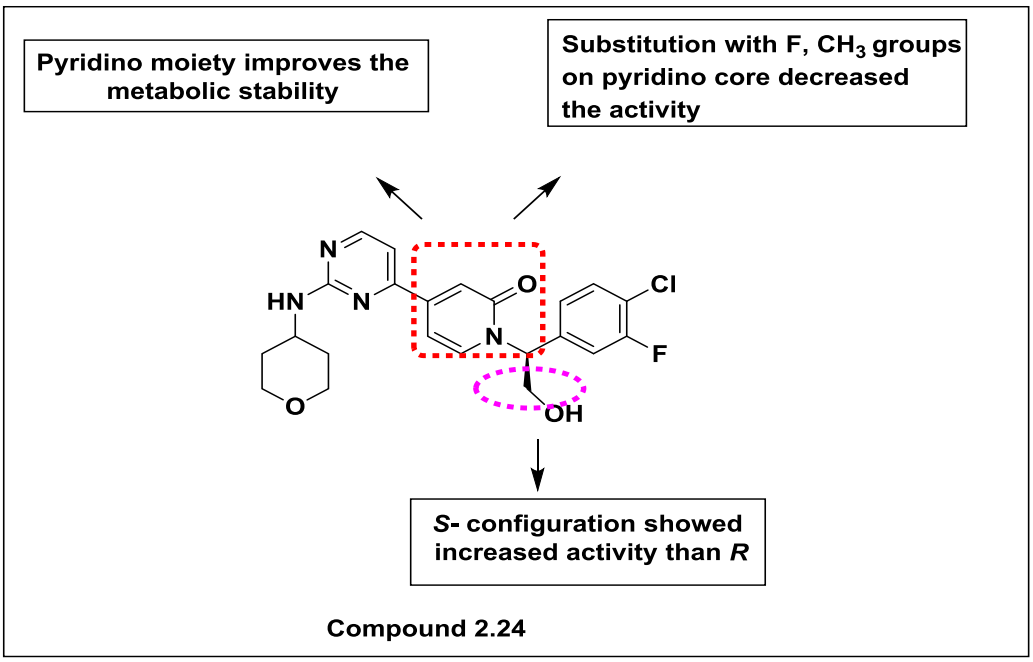

Figure 2.14. SAR study of pyridone based ERK2 inhibitor.

2.3.6. Amino pyrazole-based inhibitors

In 2016, Blake *et al.,* discovered **2.25**, an orally bioavailable ERK inhibitor. The compound was designed by replacing the tetrahydropyran ring of previously reported compound **2.21** to improve the metabolic stability of the compound (**Figure 2.15.**). Several heteroaromatic rings were substituted and evaluated for the inhibition of ERK1 and ERK2 while mechanistic potency and metabolic studies were carried out against HepG2 cells and human microsomes, respectively. Among various substitutions, compound bearing *N*-methylpyrazole showed activity in nanomolar range for both ERK1, with IC_{50} value of 6.1nM and ERK2, with IC_{50} value of 3.1nM. Additionally, it was also found metabolically stable in liver microsomes and also showed 5 times more potency than other compounds. Docking studies performed against ERK2 (PDB: 5K4I) confirmed well the binding interactions of the compound with residues like Met 108, Leu107, Gln105, and Lys114. The compound was also tested against a variety of kinases which further confirmed its selectivity (50-fold) towards ERK1. Evaluation of PK/PD and efficacy studies *in vivo* at 15, 30, and

100mg/kg disclosed that at higher dose, levels of phosphorylated p90RSK in tumors get knockdown by 87%. In the end, the compound was tested for tumor growth inhibition *via* oral administration of the drug in nude mice suffering from colorectal cancer, and results were compared with reference MEK inhibitor cobimetinib. At 100mg/kg dose, 80% inhibition of tumors was observed (Ren, Grina et al. 2015).

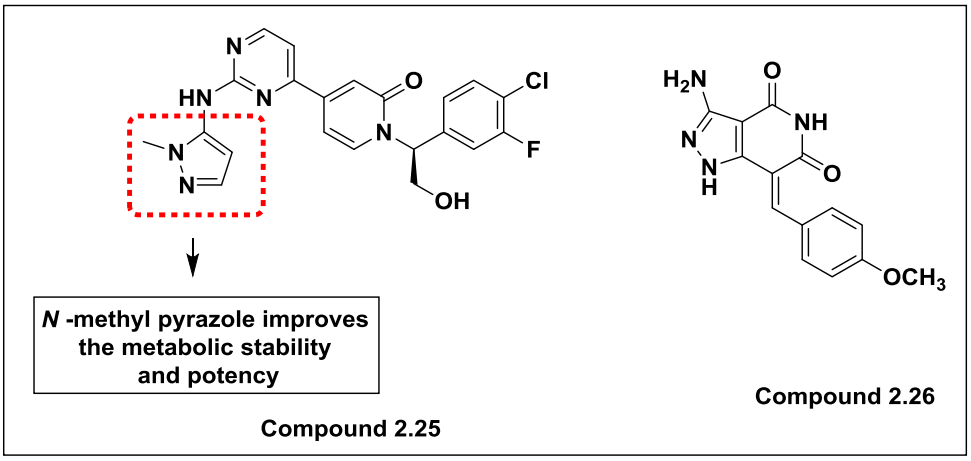

Figure 2.15. Amino pyrazole based ERK inhibitors.

Metwally *et al.*, in 2018, disclosed anti-cancer potential of novel pyrazolo[4,3-*c*]pyridine derivatives. The compounds were tested against many cancer cell lines including MCF7, HepG2 and HCT116. The molecules were synthesized using Knovenegal condensation, Michael addition and coupling reactions. Cytotoxic activity results displayed **2.26** (**Figure 2.15.**) as most active compound towards MCF7 and HepG2 with IC_{50} = 1.937 and 3.695µg/mL, respectively, in comparison to doxorubicin with IC_{50} = 2.527 and 4.749µg/ml, respectively. Binding mode analysis of **2.26** in the pocket of ERK2 (PDB: 5BUJ) showed that the compound was well occupied in a binding cavity surrounded by Tyr34 and Lys112 residues with the docking score of -6.71kcal/ mol. It also showed H-bond interactions with Met106. Docking study concluded that this molecule showed similar interaction as in reported molecules thus may act as an ERK2 inhibitor (Metwally and Deeb 2018).

2.3.7. Quinoline based inhibitors

Aly *et al.,* in 2018, disclosed anti-cancer potential of new compounds containing bis-quinolinyl naphtha quinone moiety. The anti-cancer evaluation of the compounds was performed against kinases like ERK2 and JNK2 and various cancer lines. Docking experiments, performed against the ATP-binding site of ERK2 (PDB: 4O6E), displayed the binding pattern of the compounds. Results revealed that compound **2.27 (Figure 2.16)** showed excellent inhibition of ERK2 inhibition with IC_{50} = 0.71μM. Through docking studies, it was disclosed that compound **2.27** formed three H-bonds with Ser153, Asp111, and Cys166 in the binding pocket, which were mainly responsible for the inhibition of Ets-1 phosphorylation by ERK2. Evaluation of **2.27** against 60 cancer cell lines indicated that it exhibits modest cytotoxic activity (Aly, El-Sheref et al. 2018).

Jin *et al.,* in 2019 reported quinoline derivatives of urosic acid as potent MEK 1 inhibitor. Ursolic acid, a triterpenoid was fused with rings like quinoline, oxadiazole, and thiadiazole to design various analogs to check their anticancer activity. The analogs were synthesized and tested for anti-proliferative effects against MDA-MB-231, HeLa, and SMMC-7721 cancer cell lines with etoposide as reference. Amongst all tested compounds, compound **2.28** (**Figure 2.16.**) exhibited significant activity against all three cancer cell lines having IC_{50} = 0.12 ± 0.01, 0.08 ± 0.01, and 0.34 ± 0.03μM, respectively. **2.28** was also tested against normal hepatocyte cells, QSG-7701, and observed that it possesses less cytotoxicity towards these cells (IC_{50} value =10.76 ± 0.72μM). Cell cycle analysis disclosed that **2.28** cause cell cycle arrest in G0 and G1 phase, thus showing anticancer activity. It also caused mitochondrial damage via ROS level increase and thus induced apoptosis in Hela cells. The compound was also evaluated for MEK1/2 inhibitory activity and AZD6244 was used as a positive control. The compound demonstrated good MEK1 inhibitory activity with IC_{50} = 0.064μM. Results displayed that the pERK level was decreased 74.7, 41.3, and 29.5% at concentrations of 0.05, 0.1, and 0.2μM, respectively. Furthermore, a

molecular docking study was performed against the MEK receptor (PDB: 3EQF). The compound occupied the binding activity very well with a docking score of -7.353 when compared to AZD6244 having a binding score of -7.401. The quinoline moiety of the compound **2.28** formed various hydrophobic interactions with Ala95, Leu197, and Met146. SAR study concluded that analogs bearing quinoline ring displayed improved anti-cancer activity than analogs with thiadiazole and oxadiazole. Substitution of chloro, and methoxy group on quinoline core increased activity while substitution of bulky alkyl groups in the side chain decreased the anti-cancer activity (Jin, Chen et al. 2019).

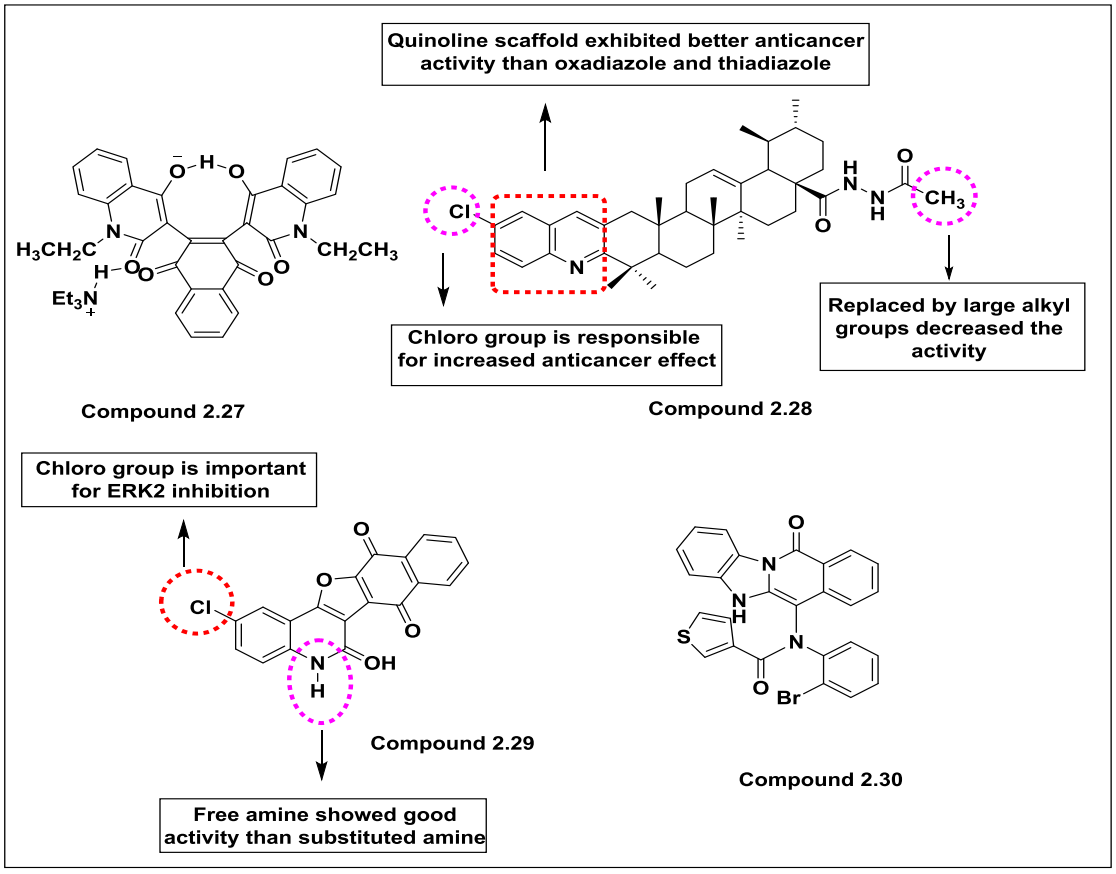

Figure 2.16. Various quinolone based ERK inhibitors along with their SAR profiles.

In 2019, Aly *et al.,* reported fused pyranoquinoline-6,7,8,13-tetraones and naphthofuroquinoline-6,7,12-triones derivatives and identified them as inhibitors of

ERK. Various analogs were prepared and tested against several cancer cell lines. Out of all the compounds, **2.29** (**Figure 2.16.**) showed more anticancer activity in comparison to others. Further, this compound was subjected to an *in-vitro* assay to determine its mechanism of action against ERK1 and ERK2. Results showed that **2.29** displayed IC_{50} = 0.5 and 0.6μM against ERK1 and ERK2, respectively. The selectivity of the compound was determined by checking its ability to inhibit other MAPK kinases such as JNK2 and p38MAPKα. The compound was found to show little activity towards them. The dose-dependent inhibition of ERK2 was observed in A375 cells, overexpressed with BRAFV600E mutation. Results displayed that the compound inhibited the phosphorylation of p90RSK and ELK (substrates of ERK) at a concentration of 25 and 10 μM, respectively, and also inhibited the proliferation in A375 cells with IC_{50} = 3.7μM. Molecular docking studies confirmed the binding mode of **2.29** in catalytic pocket of ERK (PDB: 4O6E). A hydrogen bond was observed between chlorine present on quinolone nucleus with Lys114 residue. SAR studies revealed that the existence of an EWG like chloro improves the activity while substitution with the methyl group decreased the activity. Also, the free N-H group was crucial for activity rather than substituted amine (Aly, El-Sheref et al. 2019).

In 2018, Zhang *et al.,* synthesized nine molecules containing benzimidazoisoquinoline moiety and assessed their anti-cancer potential against two glioblastoma cell lines (U87 and LN229). Out of nine molecules, compound **2.30** (**Figure 2.16.**) exhibited good anti-tumor activity and IC_{50} = 24.9μM and 27.1μM against U87 and LN229, respectively. Through flow cytometry, it was also proved that active compound mechanistically exhibits cell cycle arrest at the S-phase of glioblastoma cells. An Annexin V-FITC/PI assay disclosed that apoptosis was induced in both cells by the compound in a dose-dependent manner. Further, compound was evaluated for its inhibitory action on AKT and MAPK signaling pathways and the results revealed that **2.30** effectively inhibited the phosphorylation of c-Raf and ERK in the MAPK/ERK signaling pathway over a time period of 48 h. The compound also suppressed AKT phosphorylation, which suggested that the compound exhibit antiproliferative activity

in glioblastoma cells *via* inhibition of both MAPK and PI3K pathways (Zhang, Xu et al. 2018).

2.3.8. Guanidino based inhibitors

In 2019, Sammons *et al*., reported a new class of ERK2 inhibitors, identified through a biochemical approach including high-throughput screening which targets the D-recruitment site (DRS) and F-recruitment site (FRS) of ERK. They screened approximately 30 million compounds, followed by three phases to check their capacity of displacing fluorescent peptides from the DRS site of ERK2. Results revealed that compound bearing three cyclic guanidino groups coupled with tris(2-aminoethyl)amine displaced fluorescent peptide (FITC (fluorescein isothiocyanate) tagged D-site-containing peptide) from DRS to a greater extent than other screened compounds. During phase II, various functional groups (one position remain constant with one substitution while other positions were varied with different functional groups) were introduced on the compound and categorized as sub libraries which were further screened, resulting in the 10 active compounds. These active compounds were measured for change in anisotropy signal against inactive ERK2 and active ERK2, which revealed that FITC-X-Lig-D binds in a similar with both inactive and active form of ERK2 with Ki = 0.383 $\pm$ 0.042μM and 0.567 $\pm$ 0.122μM, respectively and selected as representative compound among all. Further, the mechanistic studies were carried out against compound **2.31** (**Figure 2.17.**) which inhibits activation of ERK2, *in vitro,* with an IC_{50} value of 9.9 ± 1.9μM, which proved that these molecules can act as inhibitors of ERK2 *via* blocking protein-protein interactions. Interaction of compounds with the DRS binding site of ERK2 was also confirmed via X-ray crystallography and NMR experiments which displayed that all top

10 compounds showed similar interaction with a common residue Asp319, thus suggesting that all inhibitors bind through a common mode (Sammons, Perry et al. 2019).

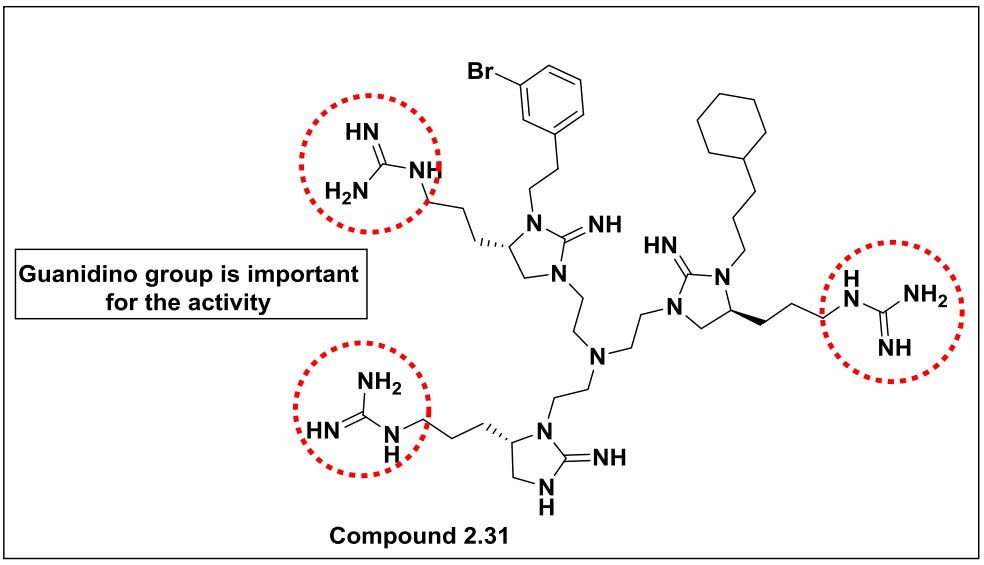

Figure 2.17. Guanidine based ERK inhibitors.

2.3.9. Indole based inhibitors

In 2019, Yu *et al.,* reported inhibitors, with dual activity against MAPK and PI3K pathway, containing substituted phenylamino indolone derivatives and evaluated against lung cancer lines. Three series of 43 compounds were designed by substituting alkenyl, alkyl, and hydroxyl groups at the 3rd position of the indolone nucleus. The designed molecules containing diphenylamine scaffold mimic the binding pattern in the allosteric pocket of MEK as present in PD0325901, a MEK inhibitor, while 3-substituted indolone conserved the PDK1 inhibitory activity as reported for BX517, a PDK1 inhibitor. The compounds were evaluated against A549 and H460, which notified that compound **2.32** (**Figure 2.18.**) was found to be most potent with IC_{50} = 1.8±0.8μM towards A549 cancer cell line. Mechanistic study towards MAPK and PI3K pathways was carried out using anti-phosphorylation activity assay with MK2206 and AZD6244 as positive controls. The compound exhibited inhibitory effects towards both pathways at a higher concentration of 2.5μM. SAR analysis revealed that compounds containing the 3-hydroxy group showed more anticancer activity than 3-alkenyl and 3-alkyl indolone compounds. Through docking studies, it was revealed that the hydroxy group formed an H-bond with residue Met219 which is

responsible for its anticancer activity whereas compounds containing 3 alkyl group lacks binding affinity towards enzyme due to free rotation of single bond and thus exhibit less anticancer activity (Yu, Chen et al. 2019).

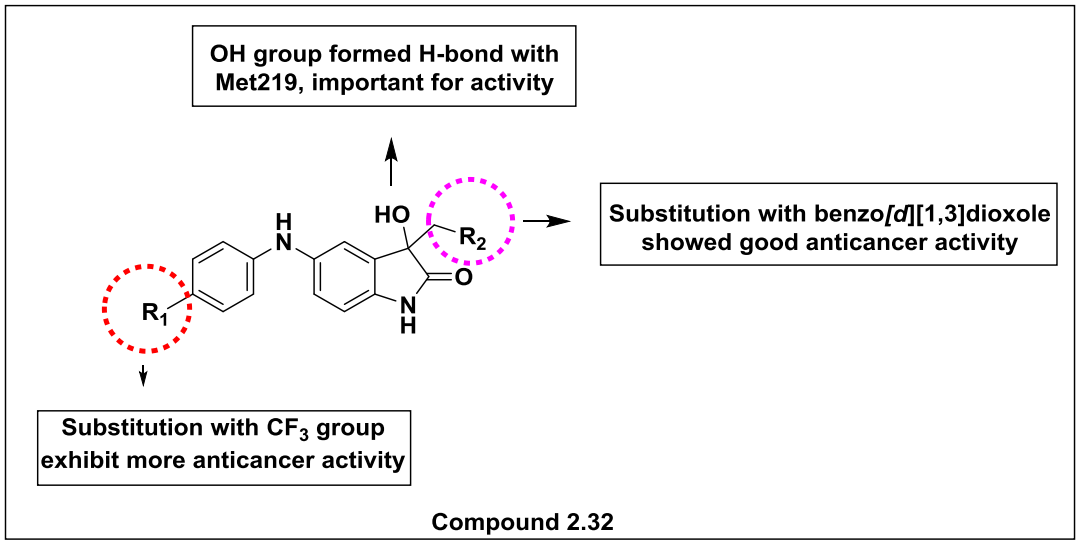

Figure 2.18. SAR profile of indole based ERK inhibitors.

2.3.10. Pyrrolidine based inhibitors

In 2018, Boga *et al.,* designed 3-substituted pyrrolidine derivatives to improve the pharmacokinetic properties of previously reported inhibitors of ERK1/2 *i.e* SCH772984 (taken as lead compound). Exhaustive lead optimization was attempted which resulted in the discovery of 3-thiomethyl pyrrolidine with 10–14 times improvement in levels of AUC in the rat at 10 mpk PO dose. Compound **2.33** (**Figure 2.19.**) also exhibited good inhibitory activity towards ERK with IC_{50} value of 7nM. Through molecular docking studies, it has been established that active compounds displayed similar hydrophobic binding interaction with Asn152, Cys164, and Try34 as that of the lead compound. SAR analysis also disclosed that substitution of pyrrolidine ring by morpholine and thiomorpholine diminished ERK2 inhibition. The *S* form, if replaced by the *R* form resulted in complete loss of activity which indicated that stereospecificity in the compound is important to preserve the ERK potency (Boga, Alhassan et al. 2018).

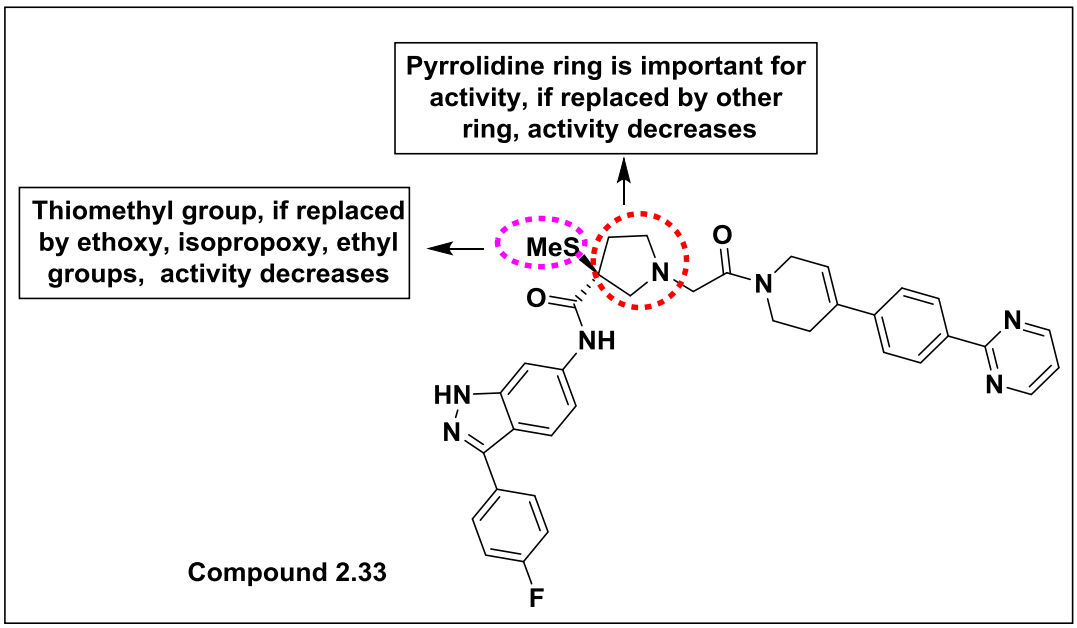

Figure 2.19. SAR profile of pyrrolidine based ERK inhibitors.

2.3.11. Indazole amide-based inhibitors

In 2016, Li *et al.,* reported designing indazole amide derivatives as inhibitors of ERK1/2 utilizing structure-guided drug design. Considering compound **2.34** as a lead molecule, optimization was done by substituting various groups on both the sides of the lead molecule. In left-hand side (LHS), substituents were introduced on pyridine rings while the right-hand side (RHS) was substituted with diverse groups (**Figure 2.20.**). Various analogs were designed and evaluated against ERK1/2 enzymatic and cellular (HT29) activity. Among all, compound **2.35** (**Figure 2.20.**) showed potent activity with IC_{50} = 9.50 ± 0.3nM and 0.48 ± 0.08μM towards ERK2 and HT29, respectively when compared to lead compound with IC_{50} = 63.3 ± 7.6nM and 9.10 ± 0.6μM towards the same. The active compound was in the *S* isomer but if replaced by the *R* isomer, there was a decrease in both enzymatic and cellular activity. SAR analysis revealed that 2-methyl pyridine and RHS wing important for the activity while methyl group in pyridine if replaced by fluoro, amino, di-methyl groups decreased the activity (Li, Liu et al. 2016).

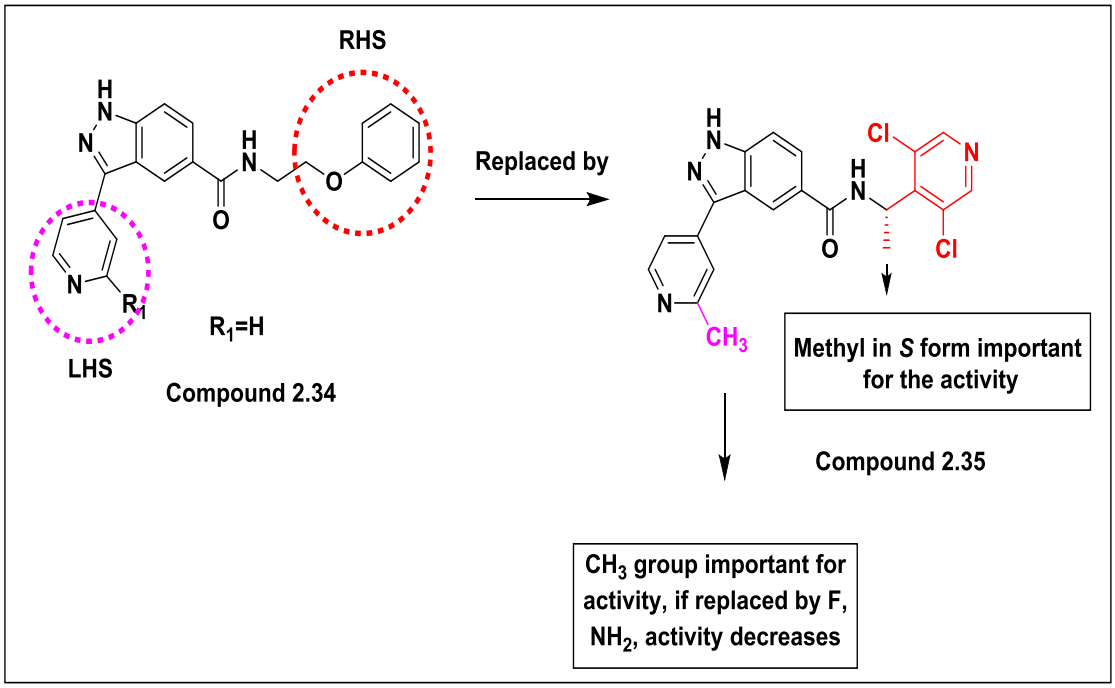

Figure 2.20. SAR profile of indazole based ERK inhibitors.

2.3.12. Imidazolinone-based inhibitors

In 2015, Awadallah *et al*., reported 1,2,4-trisubstituted imidazolinone derivatives, which were designed *via a* hybrid approach to target the p38aMAPK and ERK1/2 signaling pathway. Two pharmacophoric features were combined including diaryl substituted five-membered imidazolinone nucleus having the potential to inhibit p38MAPK and extension of the structure at 4th position of imidazolinone which contributed to ERK inhibitory activity. *In-vitro* kinase assay of synthesized compounds was performed to evaluate their ERK and p38aMAPK inhibitory potential and results were correlated with Sorafenib as standard. Results showed that compound **2.36** (**Figure 2.21.**) bearing N^1-3-methoxyphenyl-imidazolinone nucleus was more active with IC_{50} = 4.5 ± 0.3nM and 3.2 ± 0.32nM against p38Amapk and ERK2, respectively when compared to Sorafenib with IC_{50} = 37.4 ± 3.5nM and 109.5 ± 9.8nM towards p38Amapk and ERK2, respectively. The compound **2.36** was also assessed for anti-proliferative potential against nine different cancer lines which

disclosed that this molecule exhibits excellent anticancer properties against MCF7, T47D, MDA- MDAMB-435 with IC_{50} values ranging from 0.05 to 0.99µM. With these findings, it was concluded that this molecule can act as a dual inhibitor of p38Amapk and ERK2. SAR analysis revealed that 3-methoxy, 4-methoxy groups substituted on aryl ring of imidazolinone favored the activity. However, 3-methoxy increased the activity to more extent than 4-methoxy. In the extended portion of imidazolinone, the substitution of 4-CH_3 and 2-Cl on aryl ring increased the activity while groups like 2-OCH_3, 2-CH_3, 3-Cl decreased the activity (Awadallah, Abou-Seri et al. 2015).

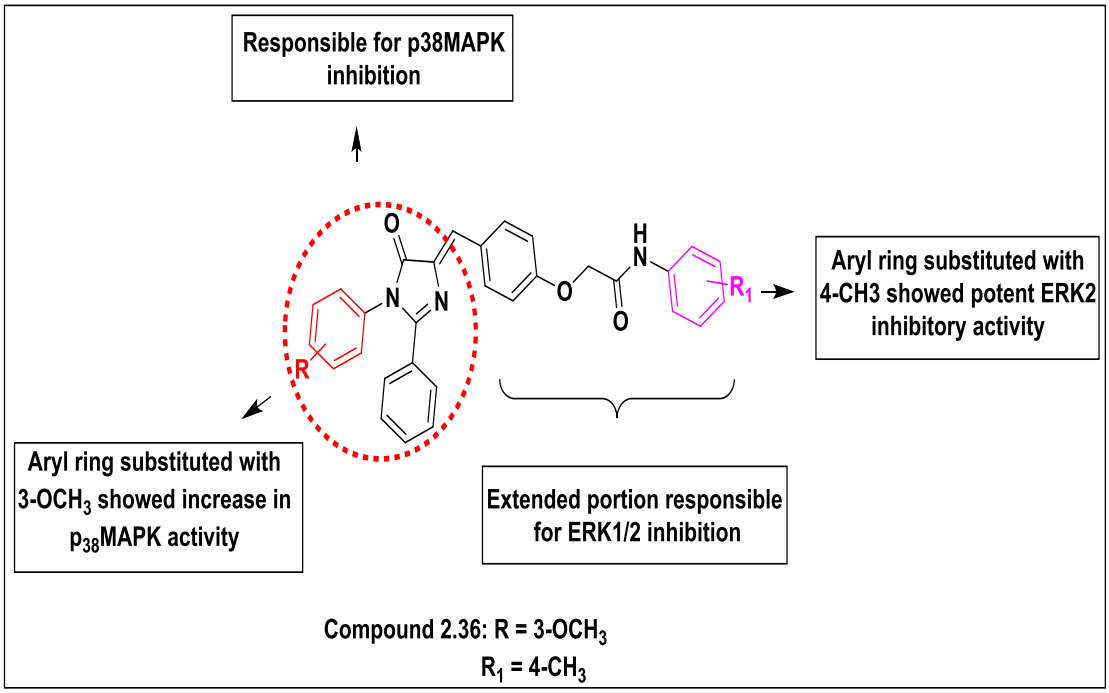

Figure 2.21. SAR profile of imidazole based ERK inhibitors.

2.3.13. Carbazole based inhibitors

In 2019, Xi and his co-workers utilized drug design approaches to find novel allosteric inhibitors of MEK. In virtual screening, out of 200,158 compounds, 13 hits were identified. The hits were evaluated for their inhibitory potential against Raf-MEK-ERK signaling cascades using LanthaScreen® Eu Kinase Binding Assay and

Selumetinib (containing biarylamine scaffold) was used as positive control. One of the hits containing naphthol scaffold was found more active with 90% inhibition of phosphorylated MEK1. Further analogues of hit compound were synthesized by replacing naphthol ring by carbazole scaffold. The carbazole ring considered as ring-closure" form of biarylamine which is important scaffold found in many ERK inhibitors. The sulphur atom in side chain of hit compound was also replaced by oxygen or a sulfonyl group (SO_2), while carboxyl group replaced by ester, amide and number of heterocycles. The synthesized analogues were then tested against Raf-MEK and MEK-ERK signaling cascades at 20 μM concentration. Among all, compound **2.37** bearing carboxylic acid group exhibited good inhibitory activity than other derivatives containing ester, amide and heterocycles, with IC_{50} value of 12.8μM, in comparison to hit with IC_{50} = 27.2μM. However, the replacement of *S* or *O* by sulfonyl group resulted in complete loss of activity (**Figure 2.22.**). Molecular docking studies of hit and active analogue were performed against allosteric site of MEK1 (PDB: 3DV3). Both compounds showed favorable interactions like carbazole ring formed π-π stacking with Phe209, carboxylic oxygen showed interactions with Lys97 while the sulfonyl oxygen of hit compound formed interaction with Lys97. However it has been found that binding pattern of active compound was more favorable than hit compound (Xi, Niu et al. 2019).

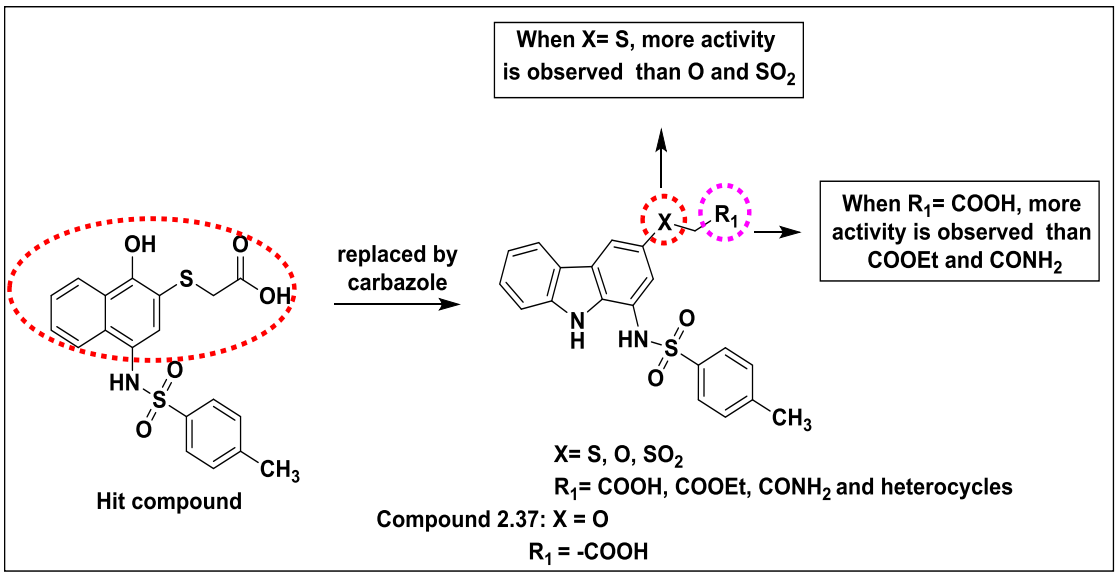

Figure 2.22. Optimization and SAR profile of carbazole based ERK inhibitors.

2.3.14. Pyrimidine-pyrrololactam based inhibitors

In 2017, Ward *et al.,* discovered a molecule containing pyrimidine-pyrrololactam moiety having potent ERK inhibitory activity. The molecule was identified using an in-house kinase selectivity database. During the process, several molecules were recognized with good ERK inhibitory action. Among all, compound **2.38** (**Figure 2.23.**) was found as the most potent active molecule with excellent inhibitory action against ERK. The molecule also possessed good *in-vitro* properties such as high solubility in water, less clearance, and good permeability. The compound was also evaluated for *in-vivo* pharmacodynamic studies against Calu-6 NSCLC model (Calu-6 cells are sensitive to ERK inhibition). The compound **2.38** showed a good response inhibiting ERK1/2 *via* reducing levels of phospho-p90RSK (pRSK), resulting in regression of tumor at the dose of 50mg/kg, once a day (Ward, Bethel et al. 2017).

2.3.15. Madecassic Acid-based inhibitors

In 2018, Valdeira *et al*., reported new madecassic acid derivatives and tested them against NCI-60 cancer cell lines. Madecassic acid, a triterpenoid obtained from

Centella asiatica exhibits many pharmacological activities, thus researchers tried to develop various analogs of madecassic acid bearing five-membered ring A. Among the tested compounds, compound **2.39** (**Figure 2.23.**) was found as most active towards B-RafV600E-mutant cell lines with a calculated mean of GI_{50} = 94.68nM against eight cancer cell lines. Further, a CellMiner^{TM} analysis assay was conducted which showed the similarity between this compound and Cobimetinib, a MEK inhibitor with r value (Pearson's correlation coefficient) = 0.71. The compound **2.39** was also evaluated against B-RafV600E mutated Colo205 colon cell line. Results declared that the compound inhibited ERK signaling cascades and decreases the level of RAF protein at the time period of 18 h. SAR studies revealed that the presence of a 2-furoyl group at C-23, *α,β*-unsaturated carbonyl and double bound at C5-C6 were important for the activity (Salvador, Gustafson et al. 2018).

2.3.16. Benzothiophene based inhibitors

In 2019, Goulielmaki *et al*., reported a new molecule containing benzothiophene nucleus with dual action towards inhibition of ERK and AKT phosphorylation. The molecule was designed *via* drug repositioning to explore this molecule against pathways like ERK/ MEK and AKT/ PI3K for anti-tumor activity. Evaluation against mutated colon cancer cell lines showed that the compound was able to reduce the cell viability by 70% at a concentration of 5µM. The compound was also tested against normal cells to determine its toxicity, which showed that the compound did not produce any effect on the normal cell, thus indicating its selectivity towards only cancer cells. Further, mechanistically it was proven that compound **2.40** (**Figure 2.23.**) inhibited MEK/ERK signaling in low micromolar concentration in the SK-MEL19 cell line. *In-vivo* activity has been also performed in nude mice induced with colon cancer. Results showed that the compound decreased the size of the tumor seven times when compared to untreated mice, hence proving the compound as a potent anticancer agent *via* inhibiting MEK signaling pathway (Goulielmaki, Assimomytis et al. 2019).

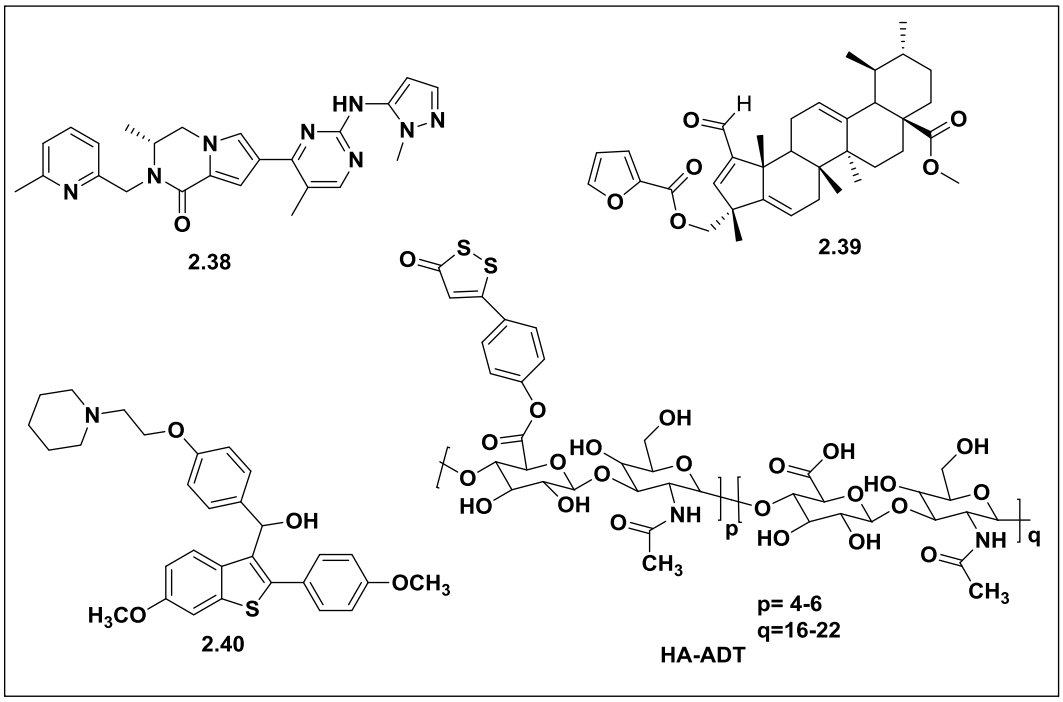

Figure 2.23. Various other reported ERK inhibitors.

2.4. Pyrimidine based ERK inhibitors

Dong *et al.,* reported 5-phenylamino-8-methylpyrido[2,3-*d*]pyrimidine-4,7(3*H*,8*H*)-dione derivatives as MEK inhibitors. A molecule named as TAK-733 (**2.41**) (**Figure 2.24.**) was found to be active both in enzymatic activity against MEK enzyme with IC_{50} = 3.2nM and against cellular ERK phosphorylation with EC_{50} = 1.9nM. Molecular docking analysis disclosed that the carbonyl of pyridone forms H-bond with NH of Ser212 whereas pyrimidinone forms an H-bond with residue Lys97 (Dong, Dougan et al. 2011). Seerden *et al*., reported the derivatives of pyrimidine fused with imidazole ring as selective p38*α* MAPK inhibitor. The compound **2.42** exhibited good MAPK inhibitory activity showing IC_{50} = 250nM in comparison to the standard JNJ7583979 with IC_{50} value = 8.5nM (**Figure 2.24.**) (Seerden, Leusink-Ionescu et al. 2014).

Liu *et al* designed a pool of 3,5-disubstituted thiazolidine-2,4-dione derivatives from a lead structure that comprised of a phenyl ring, thiazolidine and an ethylamine moiety,

and established them as inhibitors of the Raf/MEK/ERK pathway. The compounds were tested against the U937 cancer cell line. Compound **2.43** exhibited three-times more anticancer activity (IC_{50} = 3.4μM) than the lead structure (IC_{50} = 10.4μM). Furthermore, western blot analysis was performed for compound **2.43** and showed that it decreased the phosphorylated expression levels of ERKs at a concentration of 2.43μM, which indicated the correlation between growth inhibition in U937 cancer cells and blockage of ERK signaling pathway (Liu, Rao et al. 2012). Blake *et al*., reported the discovery of 5,6,7,8 tetrahydro-pyridopyrimidine as ERK2 inhibitors. The combinatorial library synthesis, high throughput screening, and molecular docking analysis resulted in the identification of **2.44**, which was further evaluated against HepG2 cancer cell line and exhibited IC_{50} = 4.4μM by inhibiting ERK-dependent phosphorylation of p90Rsk.

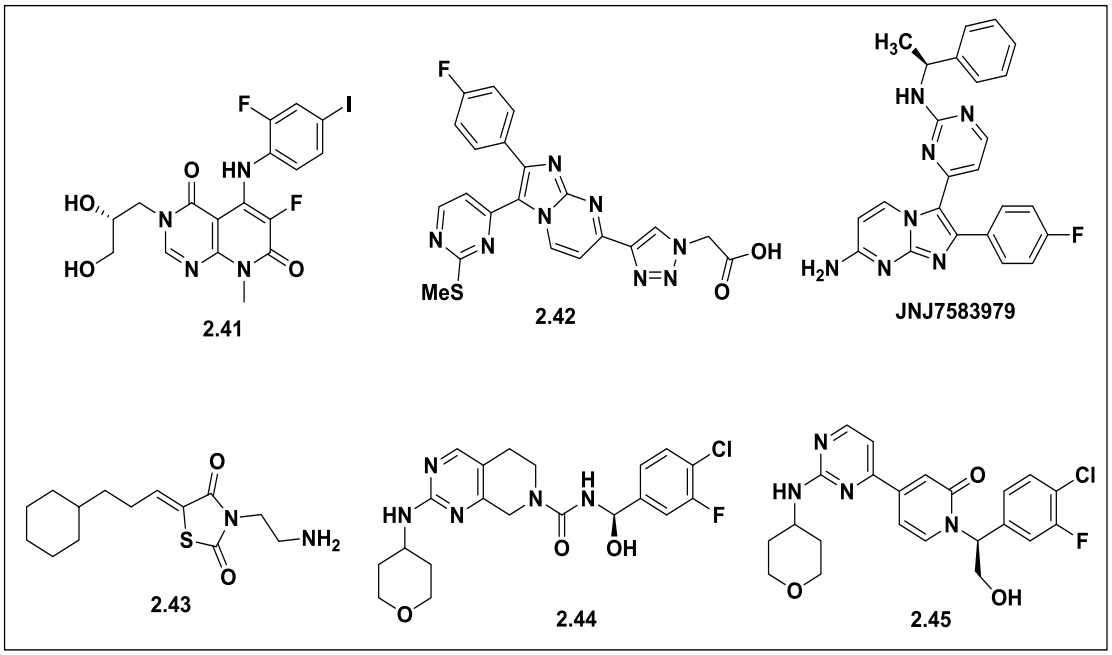

Figure 2.24. Fused pyrimidine and thiazolidine-2,4-dione derivatives as Ras/Raf/MAPK pathway inhibitors.

Docking studies also established that nitrogen of pyrimidine ring formed an H-bond with Met108 and other groups showed interactions with residues like Lys54, Gln105,

Asp167, and Glu71 (Blake, Gaudino et al. 2014). In 2015, Ren *et al* discovered some potent small molecules as ATP competitive ERK1/2 inhibitors containing pyridine and pyrimidine moiety. Through docking studies, it was observed that pyridine-based inhibitors occupied the same cavity and showed similar interactions with Lys 54. The compound **2.45** (**Figure 2.24.**) containing 3-F and 4-Cl exhibited good inhibitory activity against ERK2, especially the *S*- enantiomeric form showed 25 times more activity as compared to *the R* form (Ki = 0.3 ± 0.02nM) (Ren, Grina et al. 2015).